The DOI for this manuscript is doi: 10.1175/2011BAMS3215.1

Revision 1.5 (13 April 2010)

Measuring Total Column Water Vapor by Pointing an Infrared Thermometer at the Sky

Forrest M. Mims III

Geronimo Creek Observatory, Seguin, Texas 78155

forrest.mims@ieee.org

Lin Hartung Chambers

Climate Science Branch, Science Directorate

NASA Langley Research Center, Hampton, Virginia 23681

Lin.H.Chambers@nasa.gov

David R. Brooks

Institute for Earth Science Research and Education

Eagleville, Pennsylvania 19403

brooksdr@InstESRE.org

Corresponding Author:

Forrest M. Mims III

433 Twin Oak Road, Seguin, TX 78155

E-mail: forrest.mims@ieee.org

Abstract

A 2-year study affirms that the temperature indicated by an inexpensive ($20 to $60) IR thermometer pointed at the cloud-free zenith sky (Tz) is a proxy for total column water vapor (precipitable water or PW). Tz was measured at or near solar noon, and occasionally at night, from 8 September 2008 to 18 October 2010 at a field in South-Central Texas. PW was measured by a MICROTOPS II sun photometer. The coefficient of correlation (r^2) of PW and Tz was 0.90, and the rms difference was 3.2 mm. A comparison of Tz with PW from a GPS site 31 km NNE yielded an r^2 of 0.79, and an rms difference of 5.8 mm. An expanded study compared Tz from eight IR thermometers with PW at various times during the day and night from 17 May to 18 October 2010, mainly at the Texas site and 10 days at Hawaii's Mauna Loa Observatory. The best results were provided by two IR thermometers that yielded an r^2 of 0.96 and an rms difference with PW of 2.7 mm. The results of both the ongoing 2-year study and the 5-month comparison show that IR thermometers can measure PW with an accuracy (rms difference/mean PW) approaching 10%, the accuracy typically ascribed to sun photometers. The simpler IR method, which works day and night, can be easily mastered by students, amateur scientists and cooperative weather observers.

Capsule: A $20 infrared thermometer pointed at the cloud-free zenith sky can measure precipitable water vapor about as well as a sun photometer--and it can do so day or night.

Introduction

Water vapor is the constituent of the atmosphere most responsible for weather, the hydrological cycle and the maintenance of Earth's temperature within a range that supports life as we know it (Mockler, 1995). Furthermore, water vapor condensed on sulfate and other hygroscopic aerosols can significantly increase the aerosol optical thickness of the atmosphere (Tang, 1996).

The direct and indirect influence of water vapor on weather, climate and the environment is so important that there is significant interest in techniques for inferring its vertical distribution and its total abundance in a vertical column through the atmosphere. The latter parameter, the measurement of which is the central subject of this paper, is variously described as total column water vapor, integrated water vapor (IWV), precipitable water (PW) and integrated precipitable water (IPW). Each of these phrases specifies the depth of liquid water that would result if all the water vapor in a vertical column through the atmosphere were brought to the surface at standard temperature and pressure.

Methods of Measuring Precipitable Water

Fowle (1912) devised one of the earliest methods for measuring PW. He employed a prism spectrometer to measure the intensity of direct sunlight at the water vapor absorbing bands at 1.13 and 1.47 μm and nearby non-absorbing bands. Fowle's method led to the development of many kinds of spectrometers and sun photometers that measured PW, most of which employed pairs of silicon photodiodes and interference filters, one being preferentially transparent to the water vapor absorbing band at about 940 nm and the second transmitting a nearby reference band near 860 or 1000 nm. For example, Volz (1974) developed a handheld filter sun photometer that measured PW using a pair of appropriately filtered photodiodes. Interference filters are less costly than spectrometers, but they are subject to unpredictable drift. Mims (1992) addressed this problem by developing a filterless sun photometer that uses light-emitting diodes (LEDs) as spectrally-selective photodiodes and which has provided ongoing measurements of PW over South Central Texas since February 1990. Brooks, Mims and Roettger (2007) used LEDs in an inexpensive PW sun photometer for the GLOBE program.

Water vapor has been measured since 1930 by instrumented sounding balloons (Pettifer, 2009). PW is determined by summing the mixing ratio (grams of water vapor per kilograms of dry air) as the balloon ascends. Accuracy is affected by the performance of the temperature and humidity sensors, solar heating of these sensors and the wake effect of the ascending balloon.

Precipitable water can also be measured by a microwave radiometer tuned to frequencies emitted by liquid and gaseous water molecules (Liljegren, 1994).

Earth orbiting satellites provide several ways to monitor water vapor. The National Oceanic and Atmospheric Administration's (NOAA) Ground-Based GPS-IPW project (Gutman and Benjamin, 2001) is a network across the US and a number of other countries in which PW is inferred from the water vapor induced delay of microwave signals transmitted by Global Positioning System (GPS) satellites to ground-based receivers (Bevis *et al.,* 1992).

Various satellite instruments are used to detect the presence of water vapor. Some observe sunlight reflected from Earth at the same near-IR wavelengths monitored by ground-based sun photometers that measure water vapor by observing direct sunlight. For example, the MODIS instrument aboard the TERRA satellite measures water vapor by measuring the ratio of backscattered pairs of near-IR wavelengths (Kaufman & Gao, 1992).

Another class of satellite instruments infers the presence of water vapor by monitoring the middle-IR wavelengths that are emitted by water vapor that has absorbed sunlight. For example, the TIROS Operational Vertical Sounder (TOVS) on NOAA polar-orbiting satellites monitors upwelling radiation at 6.7, 7.3 and 8.3 μm to detect water vapor in the upper, middle and lower troposphere, respectively (Soden and Lanzante, 1996).

Various studies have compared the measurement accuracy and operational limitations of water vapor retrievals by sounding balloons and the ground and space-based instruments mentioned here (Revercomb and Coauthors, 2003).

Measuring PW with IR Detectors and Thermometers

Both clouds and water vapor absorb and re-emit radiation in discrete bands across the infrared spectrum. This permits infrared radiometers, including those configured as IR thermometers, to detect clouds, which are warmer than the clear sky, and water vapor, (Sloan, Shaw and Williams, 1955). Werner (1973) described the use of an infrared thermometer to detect clouds. The thermometer's IR sensor was a thermistor bolometer responsive to 9.5 to 11.5 μm. Today IR thermometry is used to detect the presence and temperature of clouds for meteorological research (Morris and Long, 2006). Both professional and amateur astronomers employ various IR sensors and IR thermometers to detect clouds that might interfere with their observations. For example, the Portable Cloud Sensor (Boltwood Systems Corporation) measures the sky temperature by means of a thermopile that responds to IR in a band from 8 to 14 μm (Thompson, 2005).

Idso (1982) proposed the theory of measuring water vapor pressure by pointing at the cloud-free zenith sky an infrared thermometer sensitive to a band from 10.5 to 12.5 μm. He successfully tested his theory by conducting field tests.

Recently Maghrabi and Clay (2010) described a method for estimating PW in a clear sky based on the ambient temperature and the signal from an IR radiometer designed for cloud detection (Maghrabi et al., 2009) that they described as a single-pixel IR detector. The detector was a thermopile with a spectral response of from 6.6 to >20 μm. They compared their measurements of the cloud-free zenith sky with PW measured by a GPS receiver 30 km north of their location. From October 2002 to July 2004 their IR system provided an estimate of PW with a root mean square (rms) difference of 2.31 mm from the GPS PW.

Here we describe how commercially available IR thermometers (Figure 1) can function as IR radiometers that both detect the presence of clouds and provide a means for estimating PW with an rms difference with PW given by a MICROTOPS II sun photometer of as little as 2.68 mm. This result is within 15% of that obtained by Maghrabi and Clay (2010). The IR thermometer method requires no custom electronics or expensive IR detectors and relies only on a battery-powered, handheld instrument. Nor is an ambient temperature measurement necessary, for IR thermometers incorporate temperature compensation circuitry that corrects for changes in the ambient temperature. This is usually implemented by employing a 2-element detector, one element being shielded from the source of IR being monitored and the other being exposed to the source of IR. The IR thermometer method is very inexpensive, and the second best results described below were from a $20 instrument about the size of a pocket flash memory drive (Kintrex 401).

Two-Year IR Thermometer PW Study

Geronimo Creek Observatory (GCO) is a 0.5 ha grass field in subtropical South Central Texas (29.6N 97.9W) from where a series of atmospheric measurements have been made since 1990 on most days (5,489 of 7,722 days or 71.1% of available days) at or near solar noon. The measurement suite includes PW, solar UV-B, photosynthetic radiation, the ozone layer and the aerosol optical depth at various wavelengths. From 08 September 2008 to 18 October 2010, the apparent temperature of the sky over GCO was measured with an infrared thermometer (Omega OS540) on 303 days (38.9% of the calendar days) when the zenith was cloud-free. During this two-year study, the temperature at solar noon, the usual observing time (some measurements were made at night), ranged from 2 to 35 C with a mean of 24.8 C. The dew point, which is roughly correlated with PW (Reitan, 1963), ranged from -12 to 25 C with a mean of 13 C.

In Fig. 2 the apparent zenith sky temperature (Tz), which is a proxy for the irradiance of the downwelling IR to which the OS540 responds, is plotted together with nearly simultaneous PW measurements made with a hand-held sun photometer (Solar Light MICROTOPS II, Morys *et al*., 2001). The lack of winter measurements is due to the minimum temperature measurement capability of the OS540. During winter, Tz often falls well below the -20°C minimum range of the OS540. The time series in Fig. 2 is ongoing and has become part of a suite of daily sun and atmospheric measurements.

Results of the 2-year Tz study are summarized in Table 1. Figure 3 is a scatter graph of Tz measured by the IR thermometer and PW measured by MICROTOPS II during the 2-year time series. In Fig. 3, and also in Figs. 4, 6 and 7 and the various empirical analyses that follow, no outliers have been removed, and both day and night observations are included. The correlation coefficients (r^2), rms differences and the 95% prediction bounds are from the best fits to the data provided by TableCurve™ 2D software (Jandel, 1994), all of which are of the exponential form $y = a + b \exp(-(x/c))$. In each case r^2 represents the total variance in the data that is not explained by the empirical exponential model. Note that Tz is plotted on the x axis as the independent variable instead of PW from the MICROTOPS II. This is done so that those applying the methods described herein can devise a spreadsheet in which the resulting exponential function gives PW (within the range provided by the rms difference).

The best fit to the data plotted in Fig. 3 is an exponential function that gives an r^2 of 0.90. The rms difference is 3.20 mm and the percent rms difference (rms diff/mean PW) is 10.47%. This compares favorably with the 10% error typically assigned to PW derived from sun photometer measurements (Holben et al., 2001). This makes the uncertainty all the more interesting since the PW standard is a sun photometer, and some of the scatter in the data likely originated from MICROTOPS II PW measurements that were found to be slightly dry with respect to GPS-derived PW measured at TXSM, the GPS receiver nearest GCO at San Marcos, Texas (TXSM), 31 km NNE of GCO. The mean PW measured by MICROTOPS and GPS was, respectively, 2.93 cm and 3.06 cm for all days during which Tz was measured. The MICROTOPS data might also have been biased by seasonal episodes of haze, smoke and dust and when the sun was very low in the sky. GPS measurements of PW are more accurate than those by sun photometers, with accuracy on the order of 1 mm when the required surface pressure and temperature are provided by modern surface meteorological sensors (Wolfe and Gutman, 2000).

Figure 4 is a comparison of Tz and GPS-derived PW measured at TXSM. The r^2 is 0.79, and the rms difference is 5.80 mm. This rms difference is nearly twice that of the MICROTOPS II comparison and more than twice that obtained by Maghrabi and Clay (2010) in their 21-month comparison of their IR radiometer with a GPS receiver 31 km north of their site at Adelaide, Australia, an almost identical separation distance as that between the IR thermometer measurement site at GCO and the GPS at TXSM.

As with the sun photometer comparison, various factors could have contributed to the rms differences between Tz and PW measured during the GPS comparison in Texas. For example, the comparison of IR and GPS PW by Maghrabi and Clay was made at sites with similar elevations about 10 km from the coast, which suggests a likelihood of PW being much more similar than at separated inland sites. This is supported by a comparison of one year of PW observations at TXSM and TXAN, a nearly identical GPS site 77.5 km away at San Antonio, Texas. While the difference of co-located GPS sites examined by Hagemann, et al. (2003) is under 0.7 mm, the rms difference between TXAN and TXSM of 2.22 mm is most likely due to the elevation difference between the two stations (105 m).

Another possible source of uncertainty in the GPS comparisons is that while MICROTOPS II and IR thermometer measurements were made nearly simultaneously from the same site, 30-minute averages of the measurements from the GPS site were posted online only twice an hour.

A better understanding of the greater difference with the GPS data awaits a follow up study. One possibility is to collect data over an extended time with IR thermometer connected to a data logger and mounted near a GPS receiver. A MICROTOPS II could be employed at intervals to provide a comparison of PW derived from it and the GPS (Bokoye, et al., 2007). Simultaneous optical depth measurements by the MICROTOPS II could provide a means to evaluate the possible role of airborne dust in slightly elevating Tz.

During the 2-year study in Figs. 2 and 3, dust originating from China (spring) and the Sahara Desert (summer) sometimes drifted over GCO, and it's possible that warming of the dust by sunlight might have caused a slight but false increase in PW derived from Tz. Major smoke and smog pollution events seem not to have significantly influenced the sky temperature. For example, when an IR thermometer was alternately pointed at the clear sky and a plume of smoke from a large grass fire, no clear difference in the temperature of the smoke plume and the sky was observed. This preliminary observation will be repeated under controlled conditions.

Comparison of IR Thermometers

Twenty months into the 2-year campaign, it became apparent that Tz was sufficiently well correlated with PW to justify expanding the study. On 17 May 2010, measurements by the OS540 were supplemented with measurements from four additional IR thermometers: Kintrex IRT0401 and IRT0421, Omega OS425 and Pro Exotics PE-3 (Table 2).

Results with both Kintrex IR thermometers were sufficiently good that the comparison was expanded with two additional IRT0401s and one IRT0421. (The data for these additional instruments was so well correlated with the originals that only the results for the original two are reported here.) The comparison of all eight of the 5 IR thermometer models (Table 2) was continued with from 1 to 18 observations on each of 114 days from 17 May to 18 October 2010, including day and night observations during 10 days at Hawaii's Mauna Loa Observatory. A total of 422 sets of 2,843 individual Tz and PW observations were conducted during the campaign, with 395 sets during the day and 28 at night. Figure 5 shows scatter charts that compare four of the IR thermometers used during this study.

All but one of the IR thermometers in the study can indicate temperature in degrees Celsius or Fahrenheit within one decimal point. The exception is the Kintrex IRT0401, whose readout indicates the nearest half degree (C or F). Because the Fahrenheit scale has nearly twice the resolution of the Celsius scale, all measurements were made in Fahrenheit units. With the exception of Fig. 5, temperature scales in the plots were converted to Celsius.

Some of the IR thermometers in the comparison can be adjusted to account for objects having different emissivities, while others are preset for an emissivity of 0.95, the value used for all measurements in this study. When set for an emissivity of 0.95, all the instruments gave readings within a degree or two when pointed at various objects and the bases of overhead cumulus clouds. However, sharp differences occurred when the instruments were pointed at the open sky. This was most likely caused by differing sensitivity to water vapor resultant from the various spectral responses of the IR sensors and their optics. Unfortunately, the IR spectral response for only two of the instruments was provided by the manufacturers.

The OS425 provided the most significantly different Tz readings. This instrument was added to the study due to its very narrow field of view, which would permit it to make Tz readings when clouds are near the zenith. Most IR thermometers employ a plastic Fresnel lens to focus IR from a source onto the detector. The OS525 achieves its very narrow field of view by employing a solid convex lens that appears to be composed of germanium. The zenith sky temperature is cooler than the temperature away from the zenith due to the increasing amount of water vapor in the field of view of the instrument. Thus, the very narrow field of view of the OS425 might be responsible for some of the difference in its readings. The spectral response of the sensor and the transmission differences between plastic and germanium lenses may also have contributed to the difference.

Results of the Multi-Instrument Comparison

No outliers were excluded from the analysis of Tz data collected during the multi-instrument study from 17 May to 18 October 2010, which are compared in the last 6 rows of Table 2 with PW measured by MICROTOPS II and a GPS receiver.

Tz measured by the IR thermometers during the expanded study provided rms differences from PW measured by MICROTOPS II that ranged from 2.6 to 3.5 mm. The scatter charts in Figures 6 and 7 show the results for two of the IR thermometers that provided some of the best results, the IRT0401 and IRT0421. While both these IR thermometers use the same detector, the IRT0421 looks at a much smaller region of the sky than the IRT0401. Yet both these thermometers provided remarkably similar rms differences with PW measured by MICROTOPS II, 2.72 and 2.68 mm, respectively.

The exponential functions shown in Figs. 6 and 7 can be easily used to convert Tz to PW (within the rms difference).

The GPS comparisons were much less satisfactory, with the best having an rms difference from Tz of 4.04 mm (IRT0421) and 4.11 mm (IRT0401). This greater difference is likely related to the distance to the GPS receiver (31 km). This will be explored during the planned study of a co-located IR thermometer and GPS receiver.

The most significant difference between the multi-instrument comparison and the 2-year Texas study is that the minimum T that could be measured by the OS425 IR thermometer used during the latter study was only -20° C. Therefore, the 2-year study lacks data for the coldest winter days. The IR thermometers used during the multi-instrument comparison could measure much lower temperatures (i.e., IR irradiance values), which permitted 293 measurements to be made of the very dry sky over Hawaii's Mauna Loa Observatory (MLO) from 5 to 14 June 2010. These and the Texas measurements provided a very wide range of Tz such as might be expected during a full year in temperate latitudes. For example, the maximum range of Tz measured by one of the three IRT0421 thermometers was -60.0° C to +14.2° C or 74.2°. The maximum range of Tz measured by the PE-3, which required the most time to equilibrate, was -56.1° C to +21.9° C or 78.0°. These substantial ranges, which are presumably proportional to the downwelling IR, are due entirely to water vapor. As noted above, “temperature” is a proxy for the irradiance of the downwelling IR to which the instruments respond, and differences between instruments are likely due to their respective spectral responses.

PW over MLO during this study was as low as 1 mm, which reduced Tz below the minimum measurement range of all the IR thermometers. The data from a collocated GPS receiver at MLO (MLO1) suggest that the lowest PW measureable by the IRT0401 and IRT0421 is, respectively, 1.8 mm and 3.1 mm.

The 28 sets of night Tz measurements were separately compared with PW inferred from GPS receivers. Four of the night measurements were made 37 m from a GPS receiver at MLO, and 23 were made 31 km from a GPS receiver in Texas. All night measurements with the IRT0401 and IRT0421 fell well within the scatter of day observations and were well correlated with GPS PW (r^2 = 0.989 and 0.977, respectively).

Scans across cloud-free skies at MLO and the Texas site demonstrate that the method may be used to estimate PW by pointing the IR thermometer toward the sky at known angles away from the zenith. This method will be explored to permit measurements of PW when the sun or clouds are near the zenith and when Tz falls below the minimum range of the IR thermometer on very cold, dry days and at alpine sites.

Conclusions

The studies described here demonstrate that even a very inexpensive IR thermometer pointed at a cloud-free zenith sky can infer PW with accuracy comparable to that of a sun photometer. The method works day or night so long as the thermometer is properly used and Tz is transformed to PW by an empirical calibration algorithm based on a reliable, independent means for measuring PW. Thus, an IR thermometer provides a very inexpensive instrument for meteorologists, cooperative weather observers and students to measure PW and to better understand the role of water vapor in weather and as the dominant greenhouse gas. While the requirement for a cloud-free zenith sky is a limitation, sun photometers are subject to a similar constraint, as they require a view of the sun unobstructed by clouds.

The 2-year observation program will be continued using the best of the IR thermometers identified during the multi-instrument comparison in 2010 to better understand any effects of smoke and dust on the readings and to identify any differences in day-night measurements. A protocol for measurements made away from the zenith will also be devised. Furthermore, it is hoped that a comparison of the IR method with a co-located GPS receiver can be arranged to develop an improved empirical PW calibration algorithm.

SIDEBAR 1. Trial Study at the Langley Research Center

A trial study was conducted at NASA's Langley Research Center (LaRC) on 9 days during the summer of 2010. 21 measurements of the temperature of the zenith sky were made by three observers using an Omega 0S543 IR thermometer. Near simultaneous measurements of PW were made with a MICROTOPS II. The data included major outliers unlike any observed during the 2-year study and the instrument comparisons in Texas and Hawaii. These were traced to a single operator, who apparently pointed the IR thermometer at angles well away from the zenith. When the outliers were removed, the remaining data provided the expected exponential curve, an r^2 of 0.896 and an rms difference of 1 mm from PW measured by the MICROTOPS II. The LaRC experience with unskilled operators guided the development of a protocol for making consistently reliable measurements.

SIDEBAR 2. A Protocol for Estimating PW from the Zenith Sky Temperature

For best results, select an IR thermometer with a minimum temperature of -60°C or less. Select a wide field of view (FOV) instrument for locations with generally clear to partly cloudy conditions. Select a narrow FOV instrument for cloudy regions.

The observer's back should face the sun, and the IR thermometer should be held in the observer's shadow to shield it from direct sunlight. When the sun is high in the sky, measurements should be made at mid-morning or mid-afternoon. The observer should hold the instrument so that its aperture points straight up and measure Tz by closing the appropriate switch. Tz should be recorded in a notebook along with the date, Julian day, local standard time, universal time, ambient temperature, sky condition and the operator's name. Tz should not be measured when clouds are at the zenith.

Some IR thermometers feature an alignment laser to indicate the center of the instrument's FOV. The laser should be disabled or its aperture blocked with tape to prevent the beam from striking the eyes of the operator or onlookers.

An IR thermometer can be calibrated after it has collected a series of Tz measurements during a variety of conditions. Follow these steps:

1. Transfer the data to a computer spreadsheet program. If multiple persons collected data, include their names or initials with their data.

2. Find the nearest NOAA GPS site at http://gpsmet.noaa.gov/cgi-bin/gnuplots/rti.cgi. Download the IPW (integrated PW) for the site.

3. Enter in the spreadsheet the PW measured by the GPS closest in time (UTC) to each Tz reading.

4. Make an xy chart in which Tz is plotted against the x axis and GPS PW is plotted against the y axis.

5. Use the spreadsheet to create an exponential fit to the points on the chart. Select the options for placing on the chart the coefficient of correlation and the equation representing the best fit to the data.

6. The equation for most spreadsheets will be of the form $y = e^x$, where x is Tz and y is PW. The typical spreadsheet exponential function is EXP(x), where x is the cell in which Tz is located. PW measured by the IR thermometer is calculated by entering the following into an empty cell: =a * EXP(b * cell), where the variables a and b are from the exponential fit to the data and "cell" is the address of the cell containing Tz. For example, the calibration function for an instrument used in this study (IRT0421) for a particular measurement was =1.2483*EXP(0.0241*E286), where E286 was the cell that included Tz. This function was tested with Excel™, Quattro Pro® and OpenOffice.org spreadsheets, all of which provided the same result.

7. Finally, it is important to understand that the readout of an IR thermometer pointed at the sky indicates the magnitude of IR irradiance, which should be considered a proxy for PW to which the device responds rather than the temperature of the sky. This calibration protocol must be performed for each instrument to compensate for their differing IR spectral responses.

Disclaimer and Disclosure. Trade names and product manufacturers listed in this paper are provided solely for informational purposes and imply no endorsement by the authors or by NASA. The first author discloses that he receives a royalty from Solar Light Company for sales of MICROTOPS II sun photometers.

Acknowledgments

Preparation of this paper was supported in part by a contract from the Science Directorate of NASA's Langley Research Center (LaRC). Annika Jersild assisted with the LaRC measurements. We are grateful for suggestions that greatly improved the manuscript provided by John Barnes of the Mauna Loa Observatory, Peter A. Parker of LaRC, Seth Gutman and Kirk L. Holub of NOAA's Ground-Based GPS-IPW Project, and, especially, three anonymous reviewers.

References

Bevis, Michael, Steven Businger, Thomas A. Herring, Christian Rocken, Richard A. Anthes and Randolph H. Ware, 1992: GPS Meteorology: Remote Sensing of Atmospheric Water Vapor Using the Global Positioning System. *J. Geophys. Res*, **97**, D14, 15,787-15,801.

Bokoye, A. I., A. Royer, N.T. O'Neill, P. Cliche, L.J.B. McArthur, P.M. Teillet, G. Fedosejevs and J.M. Thériault, 2003: Multisensor analysis of integrated atmospheric water vapor over Canada and Alaska. *J. Geophys. Res*., **108,** D15, 4480, doi:10.1029.

Bokoye, Amadou Idrissa, Alain Royer, Patrick Cliche, and Norm O'Neill, 2007: Calibration of Sun Radiometer–Based Atmospheric Water Vapor Retrievals Using GPS Meteorology. *J. Atmos. Ocean. Tech.*, **24**, 964-979.

Brooks, David R., Forrest M. Mims, Richard Roettger, 2007: Inexpensive Near-IR Sun Photometer for Measuring Total Column Water Vapor. *J. Atmos. Oceanic Technol*., **24**, 1268–1276.

Clay, R. W., N. R. Wild, D. J. Bird, B. R. Dawson, M. Johnston, R. Patrick, A. Sewell, 1998: A cloud monitoring system for remote sites. *Pub. Astro. Soc. Aus.*, **15**, 332–335.

Fowle, F. E., 1912: The spectroscopic determination of aqueous vapor. *Astrophys. J*., **35**, 149-162.

Gutman, S., and S. Benjamin, 2001: The Role of Ground-Based GPS Meteorological Observations in Numerical Weather Modeling. *GPS Sol.*, **4**, 16-24.

Hagemann, Stefan, Lennart Bengtsson and Gerd Gendt, 2003: On the determination of atmospheric water vapor from GPS measurements. *J.Geophy. Res.*, **108**, 4678-4692.

Holben, B.N. and Coauthors, 2001: An emerging ground-based aerosol climatology: Aerosol optical depth from AERONET. *J. Geophy. Res.,* **106**, D11, 12,067–12,097.

Idso, Sherwood B., 1982: Humidity Measurement by Infrared Thermometry. *Rem. Sens. Env.,* **12**, 87-91.

Jandel Scientific, 1994: *TableCurve™ 2D User's Manual*.

Kaufman, Y. J., and B. C. Gao, 1992: Remote sensing of water vapor in the near IR from EOS/MODIS. *IEEE Trans. Geosci. Rem. Sens.*, **30**, 871-884.

Liljegren, J. C., 1994: Two-channel microwave radiometer for observations of total column precipitable water vapor and cloud liquid water path. In *Proc. Fifth Sym. Global Change Studies*, Amer. Meteor. Soc., Nashville, Tenn., January 23-28, 262-269.

Maghrabi, A. H., R. W. Clay, B. Dawson and N. Wild, 2009: Design and development of a simple infrared monitor for cloud detection. *Energy Conser. Manag.*, **50**, 11, 2732–2737.

Maghrabi, A. and R. Clay, 2010: Precipitable water vapour estimation on the basis of sky temperatures measured by a single-pixel IR detector and screen temperatures under clear skies. *Meteor. App.*, **17**, 279–286.

Mims III, F. M., 1992: Sun Photometer with Light-Emitting Diodes as Spectrally Selective Detectors. *App. Opt.* **31**, 33, 6965-6967.

Mockler, Susan Bucci, 1995: *Special Report: Water Vapor in the Climate System.* AGU.

Morris, V., C. Long and D. Nelson, 2006: Deployment of an Infrared Thermometer Network at the Atmospheric Radiation Measurement Program Southern Great Plains Climate Research Facility. *Proc. of the Sixteenth Atmos. Rad. (ARM) Sci. Team Meet.*, U.S. Dept. Energy, Richland, Washington.

Morys, Marian, Forrest M. Mims III, Scott Hagerup, Stanley Anderson, Aaron Baker, Jesse Kia and Travis Walkup, 2001: Design, calibration and performance of MICROTOPS II handheld ozone monitor and Sun photometer. *J. of Geophy. Research*, **106**, 14,573-14,582.

Pettifer, Richard, 2009: From Observations to Forecasts - Part 2. The development of in situ upper air measurements. *Weather*, **64**, 302-308.

Reitan, C.H., 1963: Surface dew point and water vapor aloft. *J. Ap. Meteor.*, **2**, 776-779.

Revercomb, H. E., and Coauthors, 2003: The Arm Program's Water Vapor Intensive Observation Periods. *Bull. Amer. Meteor. Soc.*, **84**, 217–236.

Sloan, Raymond, John H. Shaw and Dudley Williams, 1955: Infrared Emission Spectrum of the Atmosphere. *Opt. Soc. Am*., **45**, 455-457.

Soden, Brian J., John R. Lanzante, 1996: An Assessment of Satellite and Radiosonde Climatologies of Upper-Tropospheric Water Vapor. *J. Climate*, **9**, 1235–1250.

Tang, I.N., 1996: Chemical and size effects of hygroscopic aerosols on light scattering coefficients. *J. of Geophy. Res.*, **101**, 19245-19250.

Thompson, Marcus, 2005. Boltwood Cloud Sensor. Cloudy Nights Telescope Reviews. (Accessed at http://www.cloudynights.com/item.php?item_id=1261)

Volz, F. E., 1974: Economical multispectral sun photometer for measurements of aerosol extinction from .44 microns to 1.6 microns and precipitable water. *Appl. Opt.*, **13**, 1732-1733.

Werner, C., 1973: Automatic Cloud Cover Indicator System. *J. Appl. Meteor.*, **12**, 1394.

Wolfe, Daniele E. and Gutman, Seth I., 2000: Developing an Operational, Surface-Based, GPS, Water Vapor Observing System for NOAA: Network Design and Results. *J. Atmos. Ocean. Tech.*, **17**, 426-440.

Table Captions

Table 1. Results of a 2-year comparison of Tz and PW measured by a co-located MICROTOPS II sun photometer and a GPS receiver 31 km NNE.

Table 2. Key manufacturer specifications of five models of commercially available IR thermometers used in the expanded study (17 May to 18 October 2010). The last 6 rows give the comparison of Tz readings indicated by these thermometers and PW measured by a co-located MICROTOPS II sun photometer (SP) and GPS receivers at Mauna Loa Observatory and 31 km NNE of the Texas site.

Figure Captions

Figure 1. The 5 models of IR thermometers used in the precipitable water vapor study.

Figure 2. A two-year (08 Sep 2008 to 18 Oct 2010) time series of the apparent temperature of the cloud-free zenith sky (Tz, red) indicated by an IR thermometer and precipitable water (PW, blue) measured by a MICROTOPS II sun photometer at Geronimo Creek Observatory, a field in South Central Texas (29.61N 97.93W). This plot shows how Tz is a proxy for PW.

Figure 3. Scatter plot of Tz and PW retrievals during a 2-year study, with PW being that measured by a MICROTOPS II. The red line is the best fit to the data (exponential a,b,c). The dashed lines are the 95% prediction bounds.

Figure 4. Scatter plot of Tz and PW retrievals during a 2-year study, with PW being that measured by a GPS 31 km NNE of the observation site. The red line is the best fit to the data (exponential a,b,c). The dashed lines are the 95% prediction bounds.

Figure 5. Scatter plots comparing Tz measured by four IR thermometers during an expanded study from 17 May to 05 September 2010. The suffixes 1 and 2 indicate different versions of the same instrument model. Temperatures below -5° F were measured at the Mauna Loa Observatory, where the sky is often exceptionally dry. The temperatures are given in the degrees Fahrenheit in which they were measured to provide higher resolution than the Celsius scale.

Figure 6. Scatter plot of Tz measured by a miniature IRT0401 IR thermometer and PW measured by MICROTOPS II during the expanded study from 17 May to 18 October 2010. The rms difference is 2.72 mm and the rms difference from the mean PW is 10.96%. As in Figs. 3 and 4, the red line is the best fit to the data (exponential a,b,c), and the dashed lines are the 95% prediction bounds.

Figure 7. Scatter plot of Tz measured by an IRT0421 IR thermometer and PW measured by MICROTOPS II during the multi-instrument comparison from 17 May to 18 October 2010. The rms difference is 2.68 mm and the rms difference from the mean PW is 10.27%. The red line is the best fit to the data (exponential a,b,c).

Table 1. Results of a 2-year comparison of Tz and PW measured by a co-located MICROTOPS II sun photometer and a GPS receiver 31 km NNE.

OS540	MICROTOPS	GPS
r^2	0.898	0.793
RMS difference	3.20 mm	5.80 mm
RMS dif/Mean	10.47%	18.21%

EDITOR: Table 2 continues on the next page.

Table 2. Key manufacturer specifications of five models of commercially available IR thermometers used in the expanded study (17 May to 18 October 2010). The last 6 rows give the comparison of Tz readings indicated by these thermometers and PW measured by a co-located MICROTOPS II sun photometer (SP) and GPS receivers at Mauna Loa Observatory and 31 km NNE of the Texas site.

Model	IRT0401	OS540	PE-3	IRT0421	OS425
Manufacturer	Kintrex	Omega	ProExotics	Kintrex	Omega
Minimum T	-55°C (-67°F)	-20°C (-4°F)	-60°C (-76°F)	-60°C (-76°F)	-60°C (-76°F)
Accuracy	+/-2% or 4°F (2°C)	+/-2%	+/-2%	+/-1.0°C (1.8°F)	+/-1.0°C (1.8°F)
Distance:Spot	1:1	8:1	8:1	12:1	50:1
Field of View	53.1°	7.2°	7.2°	4.8°	1.1°
Emissivity	0.95	0.95	Adjustable	0.95	Adjustable
Spectral Range	5 to 14 µm	Unavailable	Unavailable	5 to 14 µm	Unavailable
	0.964	0.874	0.896	0.960	0.916

MICROTOPS: r^2					
MICROTOPS: RMS difference	2.72 mm	3.42 mm	3.82 mm	2.68 mm	2.77 mm
MICROTOPS: RMS dif/Mean	10.96%	10.47%	13.00%	10.27%	8.68%
GPS: r^2	0.944	0.824	0.807	0.936	0.881
GPS: RMS difference	4.12 mm	4.74 mm	6.26 mm	4.08 mm	3.85 mm
GPS: RMS dif/Mean	15.58%	12.78%	18.41%	14.00%	10.50%

Figure 1. Figure 1. The 5 models of IR thermometers used in the precipitable water vapor study.

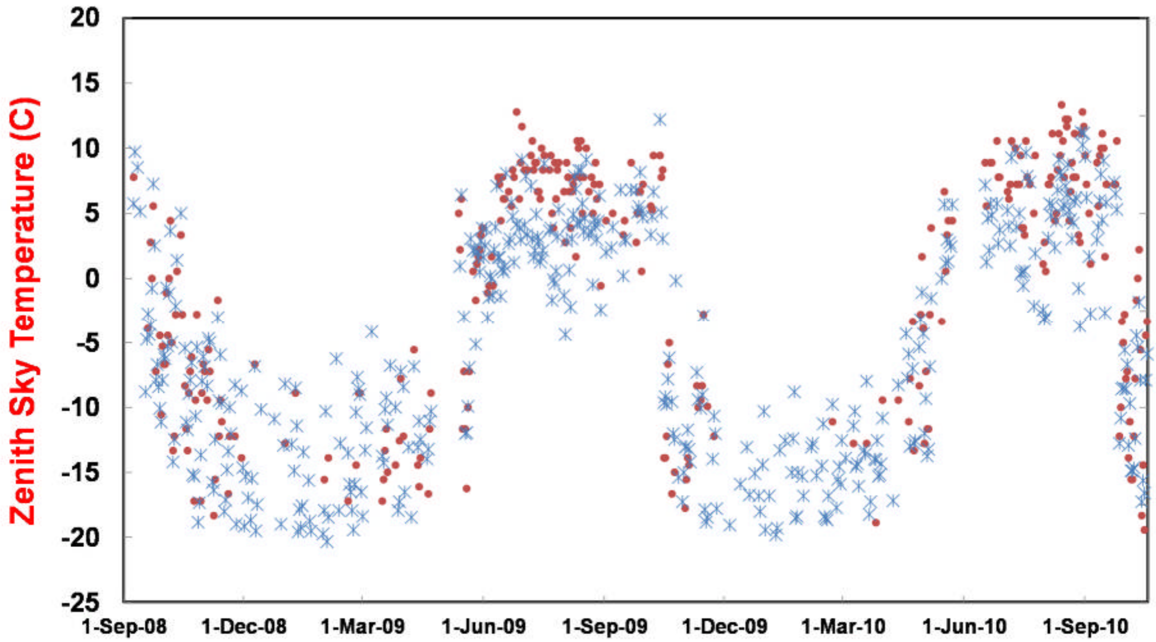

Figure 2. A two-year (08 Sep 2008 to 18 Oct 2010) time series of the apparent temperature of the cloud-free zenith sky (Tz, red) indicated by an IR thermometer and precipitable water (PW, blue) measured by a MICROTOPS II sun photometer at Geronimo Creek Observatory in South Central Texas (29.61N 97.93W). This plot shows how Tz is a proxy for PW.

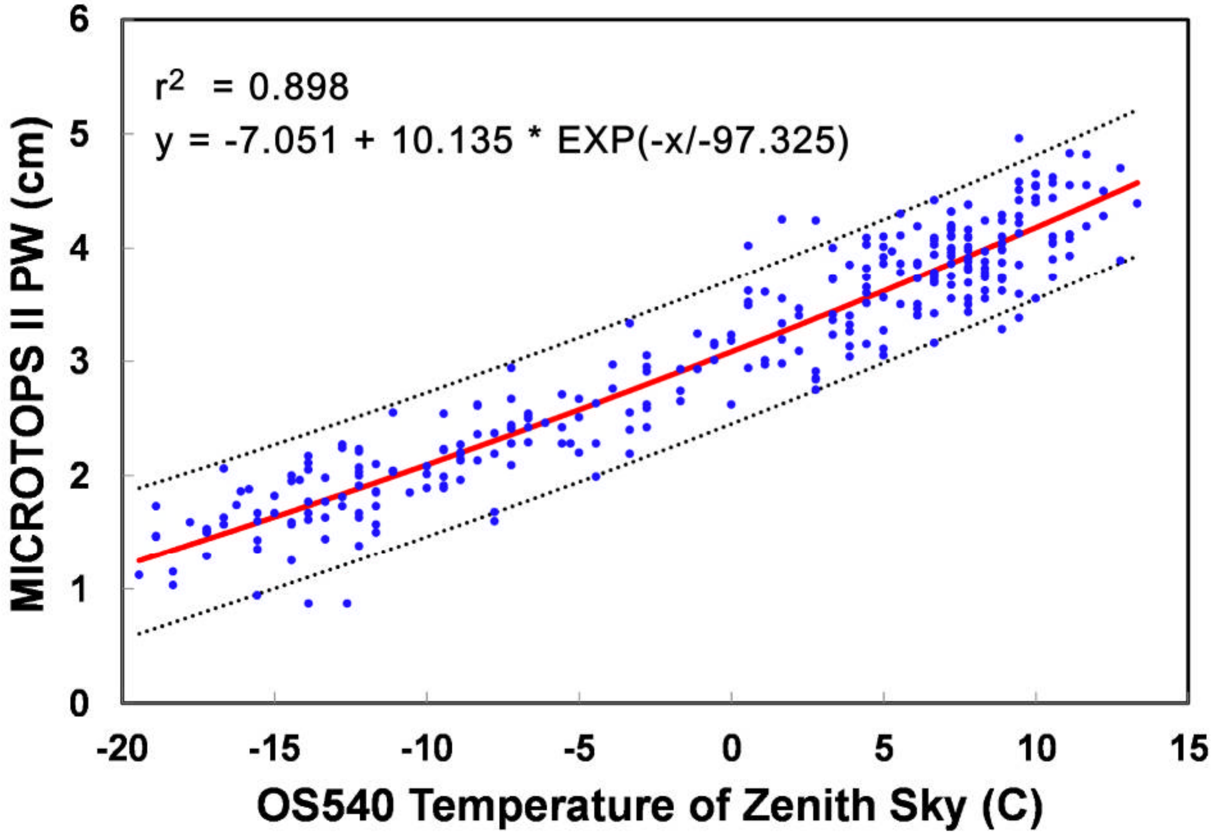

Figure 3. Scatter plot of Tz and PW retrievals during a 2-year study, with PW being that measured by a MICROTOPS II. The red line is the best fit to the data (exponential a,b,c). The dashed lines are the 95% prediction bounds.

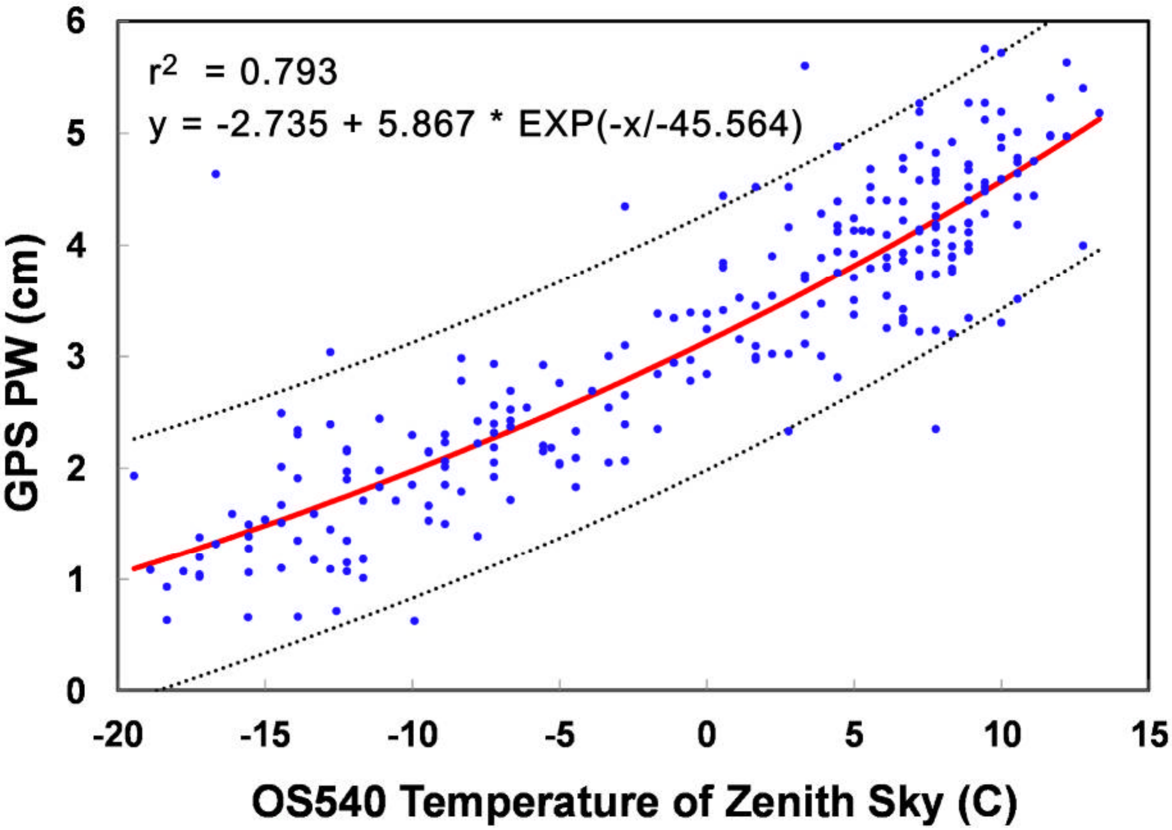

Figure 4. Scatter plot of Tz and PW retrievals during a 2-year study, with PW being that measured by a GPS 31 km NNE of the observation site. The red line is the best fit to the data (exponential a,b,c). The dashed lines are the 95% prediction bounds.

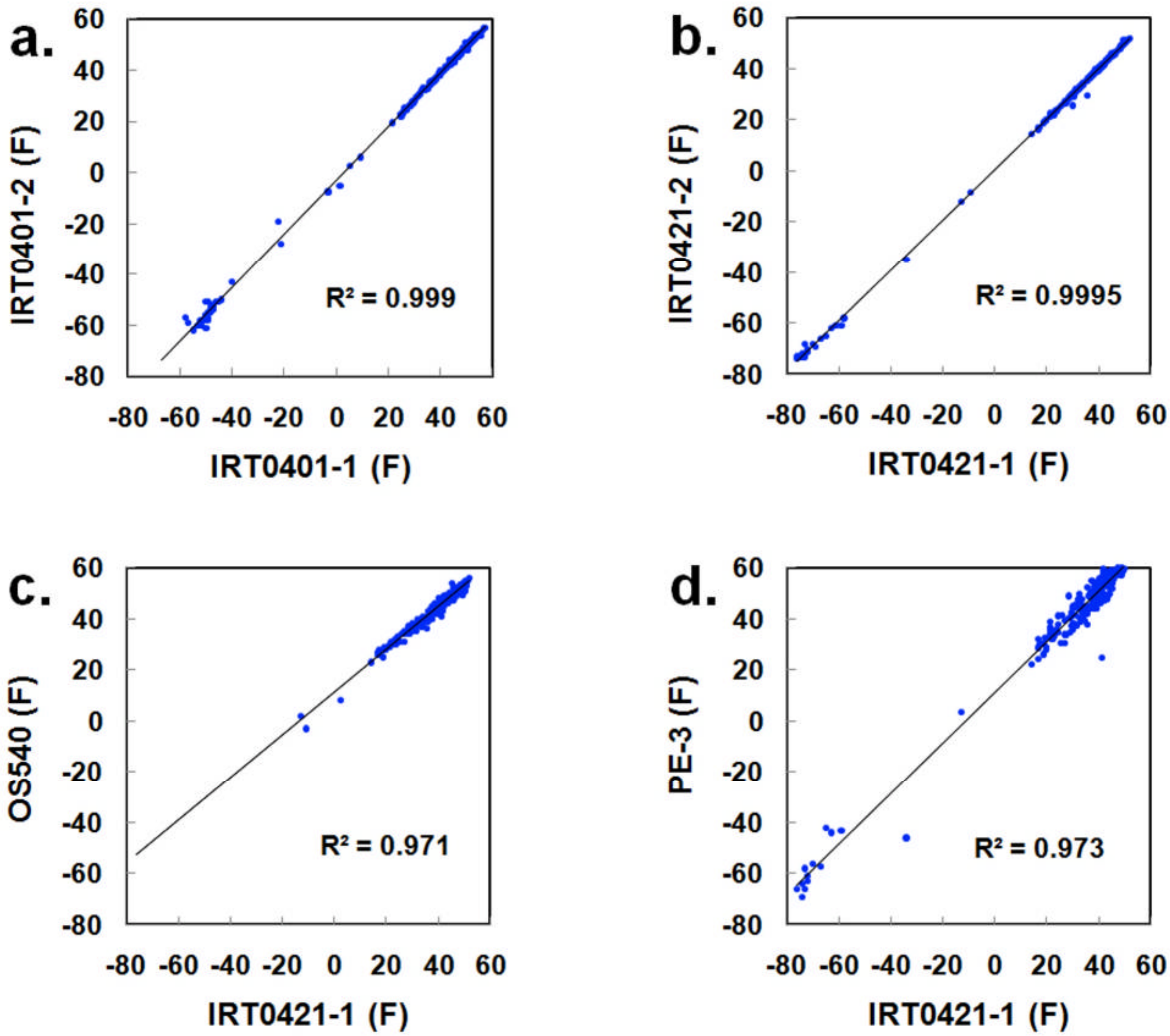

Figure 5. Scatter plots comparing Tz measured by four IR thermometers during an expanded study from 17 May to 05 September 2010. The suffixes 1 and 2 indicate different versions of the same instrument model. Temperatures below -5° F were measured at the Mauna Loa Observatory, where the sky is often exceptionally dry. The temperatures are given in the degrees Fahrenheit in which they were measured to provide higher resolution than the Celsius scale.

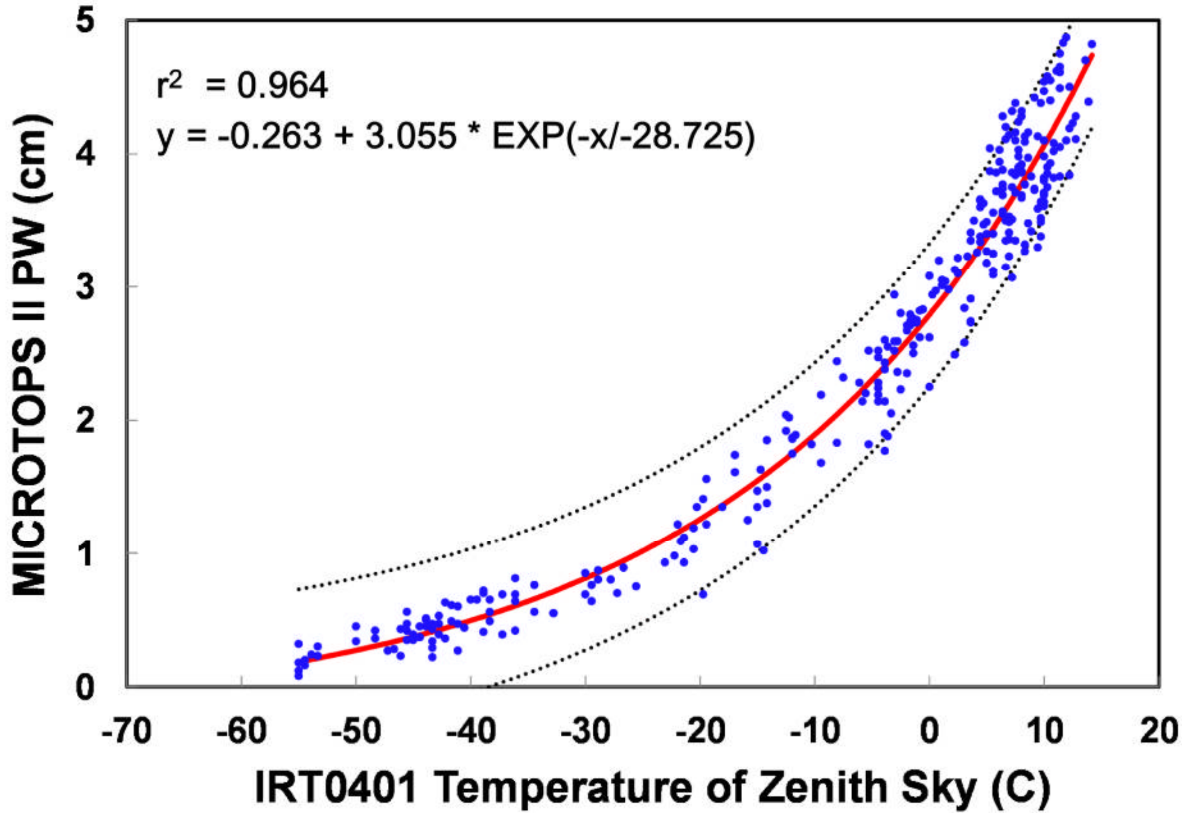

Figure 6. Scatter plot of Tz measured by a miniature IRT0401 IR thermometer and PW measured by MICROTOPS II during the expanded study from 17 May to 18 October 2010. The rms difference is 2.72 mm and the rms difference from the mean PW is 10.96%. As in Figs. 3 and 4, the red line is the best fit to the data (exponential a,b,c), and the dashed lines are the 95% prediction bounds.

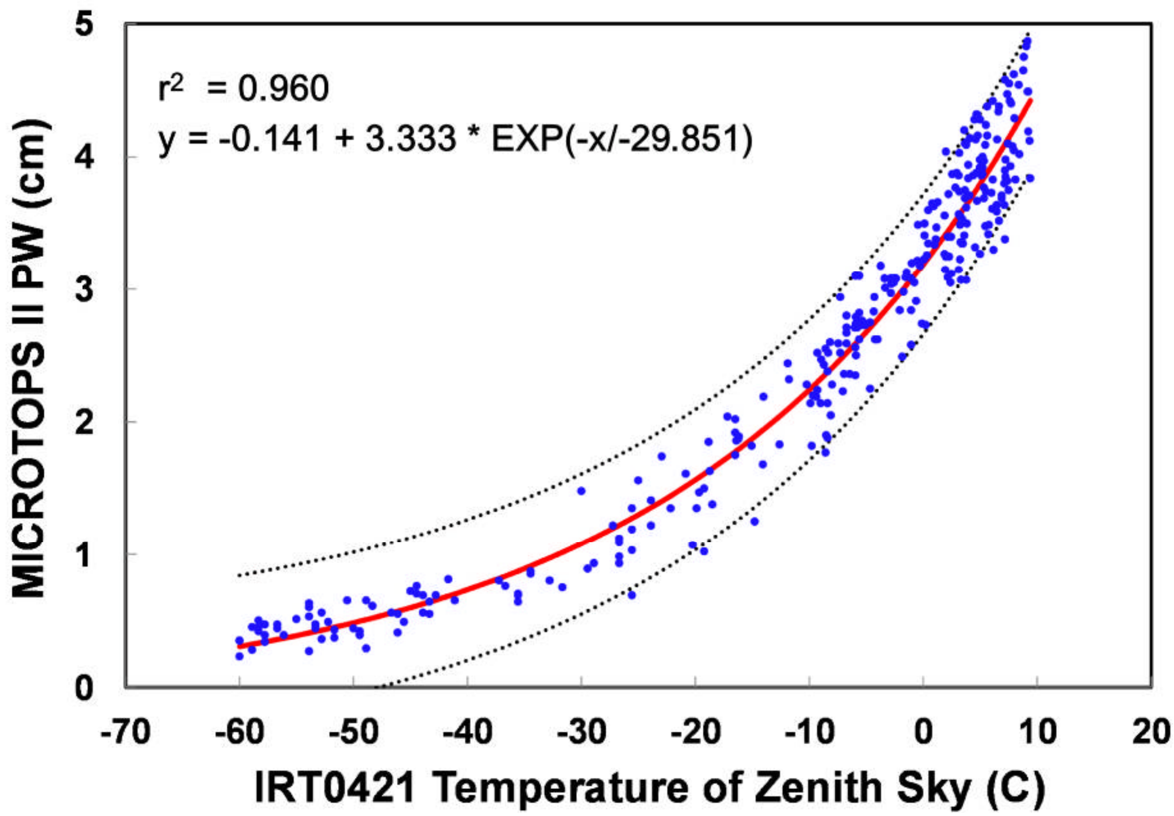

Figure 7. Scatter plot of Tz measured by an IRT0421 IR thermometer and PW measured by MICROTOPS II during the multi-instrument comparison from 17 May to 18 October 2010. The rms difference is 2.68 mm and the rms difference from the mean PW is 10.27%. The red line is the best fit to the data (exponential a,b,c).